Selective neural activation in a histologically derived model of peripheral nerve

2011 J. Neural Eng. 8 036009

(http://iopscience.iop.org/1741-2552/8/3/036009)

J. Neural Eng. **8** (2011) 036009 (9pp) doi:10.1088/1741-2560/8/3/036009

Selective neural activation in a histologically derived model of peripheral nerve

Christopher R Butson[1,5], Ian O Miller[2], Richard A Normann[3] and Gregory A Clark[3,4]

[1] Departments of Neurology & Neurosurgery, Medical College of Wisconsin, Milwaukee, WI, USA
[2] Department of Neurology, Miami Children's Hospital, Miami, FL, USA
[3] Department of Bioengineering, University of Utah, Salt Lake City, UT, USA
[4] School of Computing, University of Utah, Salt Lake City, UT, USA

E-mail: cbutson@mcw.edu

Received 5 November 2010
Accepted for publication 9 March 2011
Published 11 April 2011
Online at stacks.iop.org/JNE/8/036009

Abstract

Functional electrical stimulation (FES) is a general term for therapeutic methods that use electrical stimulation to aid or replace lost ability. For FES systems that communicate with the nervous system, one critical component is the electrode interface through which the machine–body information transfer must occur. In this paper, we examine the influence of inhomogeneous tissue conductivities and positions of nodes of Ranvier on activation of myelinated axons for neuromuscular control as a function of electrode configuration. To evaluate these effects, we developed a high-resolution bioelectric model of a fascicle from a stained cross-section of cat sciatic nerve. The model was constructed by digitizing a fixed specimen of peripheral nerve, extruding the image along the axis of the nerve, and assigning each anatomical component to one of several different tissue types. Electrodes were represented by current sources in monopolar, transverse bipolar, and longitudinal bipolar configurations; neural activation was determined using coupled field–neuron simulations with myelinated axon cable models. We found that the use of an isotropic tissue medium overestimated neural activation thresholds compared with the use of physiologically based, inhomogeneous tissue medium, even after controlling for mean impedance levels. Additionally, the positions of the cathodic sources relative to the nodes of Ranvier had substantial effects on activation, and these effects were modulated by the electrode configuration. Our results indicate that physiologically based tissue properties cause considerable variability in the neural response, and the inclusion of these properties is an important component in accurately predicting activation. The results are used to suggest new electrode designs to enable selective stimulation of small diameter fibers.

Introduction

Functional electrical stimulation (FES) is a general term for techniques that are used to restore lost function due to neurological deficits. Such methods have been in use for over two millennia, beginning with the use of the torpedo fish to treat headache (Hambrecht and Reswick 1977). Five basic life activities that are now candidates for FES are breathing, eating, defecating, urinating and moving (Peckham and Gray 1996, Wieler *et al* 1999). The primary goals of FES are to reduce morbidity and mortality, and to improve quality of life for the patient. One factor that complicates the clinical application of this approach is the inability to predict the distribution of neuronal activation around an electrode. As a result, programming a peripheral stimulation system can

[5] Author to whom any correspondence should be addressed.

require a trial-and-error approach that is time consuming, inefficient, and that may not provide maximal restoration of function.

In this paper we examine the body–machine interface that is a component of FES systems for neuromuscular control. The primary goal of these systems is to provide precise motor control to restore movement with minimal muscle fatigue. However, in spite of many improvements in FES technologies, complete restoration of complex motor function is not yet possible. Generation of graceful yet powerful muscle forces via stimulation of peripheral nerve is complicated by nonselective stimulus mechanisms, as well as indeterminate voltage and current values required for optimal recruitment of individual neurons. In order to be effective, these systems must recruit small axons before large ones (i.e. reproduce the physiological recruitment order), enable spatial selectivity within the nerve and muscles, and accomplish these objectives with minimal charge injection. One advantage of neural stimulation for FES is that it requires far less energy than direct stimulation of muscle. However, one limitation of neural stimulation is that neurons are activated in the inverse, rather than physiological, recruitment order. Large-diameter axons are activated before small-diameter ones, and because there is a direct correlation between myelinated axon diameter and motor unit size, this results in contraction of large, fast-fatigable motor units first. As a result, rather than creating smooth, graceful movements, artificially stimulated movements tend to be coarse, lack fine motor capacity and fatigue quickly.

Electrical stimulation via implanted microelectrodes permits excitation of small, highly localized populations of neurons, and allows access to features of neuronal organization that are not accessible with larger electrodes implanted on the surface of the brain or spinal cord (McIntyre and Grill 2001). Several groups have used computational models of peripheral nerve to examine the effects of different stimulation motifs. McNeal used a model of extracellular stimulation to induce subthreshold and suprathreshold responses of myelinated fibers for finite duration pulses (McNeal 1976), and later Veltink *et al* constructed a model of hexagonal cylinders to determine activation in a nerve model using the same activation detection algorithm (Veltink *et al* 1989). Temporal properties of the stimulation waveform such as pulse width or subthreshold depolarization on recruitment order have been investigated (Grill and Mortimer 1996, 1997). More recently, physiological recruitment order has been investigated by varying the electrode spacing and number of anodic and cathodic band electrodes (Lertmanorat and Durand 2004a, 2004b). Lastly, modeling studies have been conducted to examine neural activation as a function of changes in conductivity ratios (Grill 1999), perineurium geometry (Grinberg *et al* 2008) and the effects of fascicular organization on stimulation effectiveness (Brill *et al* 2009, Durand *et al* 2009, Schiefer *et al* 2008).

In this paper we focus on arrays of penetrating electrodes such as the Utah Electrode Array, which have the potential to provide a high degree of spatial and fiber diameter selectivity in the neural response (Branner and Normann 2000, Normann 2007, Dowden *et al* 2009, 2010). The purpose of this paper is to address two basic questions regarding neural stimulation. First, what are the effects of physiological properties such as tissue conductivity or position of nodes of Ranvier on the neural response to stimulation? There are many sources of variability in the responses to stimulation, but few of these have been parameterized. Second, how is the neural response modulated by the electrode design? To address these questions, we built a three-dimensional (3D), biophysically realistic model of a fascicle from a stained cross-section of cat sciatic nerve. This model contains several important features that have not been included in previous efforts. The anatomical model includes representation of several potentially important structures: the epineurium that envelops the nerve trunk; the perineurium that surrounds the individual fascicles; and the endoneurium, which surrounds the axons and consists of Schwann cells and connective tissue matrix. Because of the longitudinal arrangement of myelin in the fascicle, current is able to flow more easily in the axial direction than across the nerve, making the bulk intrafascicular conductivity anisotropic. We took this analysis a step further by explicitly constructing the nerve fibers in the extracellular milieu. We sought to determine whether the presence of physiologically based, 3D tissue properties has an effect on the electric field in the tissue medium, and in turn on neural activation. We then used this information to suggest more effective stimulation strategies.

Methods

The methods used to model physiological systems are composed of a basic set of governing equations, techniques and solution methods. In the context of neural field modeling, these methods include the construction of the anatomical model, specification of material properties, numerical approximation of biophysical field equations, and the solution to large systems of equations (Johnson 1997). We developed a high-resolution bioelectric field model of an individual fascicle that was derived from a stained cross-section of cat sciatic nerve. The model included identification of several different tissue types with individual conductivities. Neural activation as a function of electrode configuration was determined using field–neuron simulations in which the voltage from the field model is interpolated onto cable model neurons with detailed representations of the cell membrane, myelin and nodes of Ranvier. Activation was calculated as a function of the conductivity model, electrode configuration and position of nodes of Ranvier.

Anatomical model

We first constructed an anatomical model from a specimen of cat sciatic nerve prepared with Richardson's stain, which is specific for myelin and other prominent cellular structures. An image of the nerve was obtained with an image capturing microscope. The specimen was 4.5 mm wide, and was scanned at 72× power (non oil-immersion). An individual fascicle was selected from within the nerve for construction of the 3D

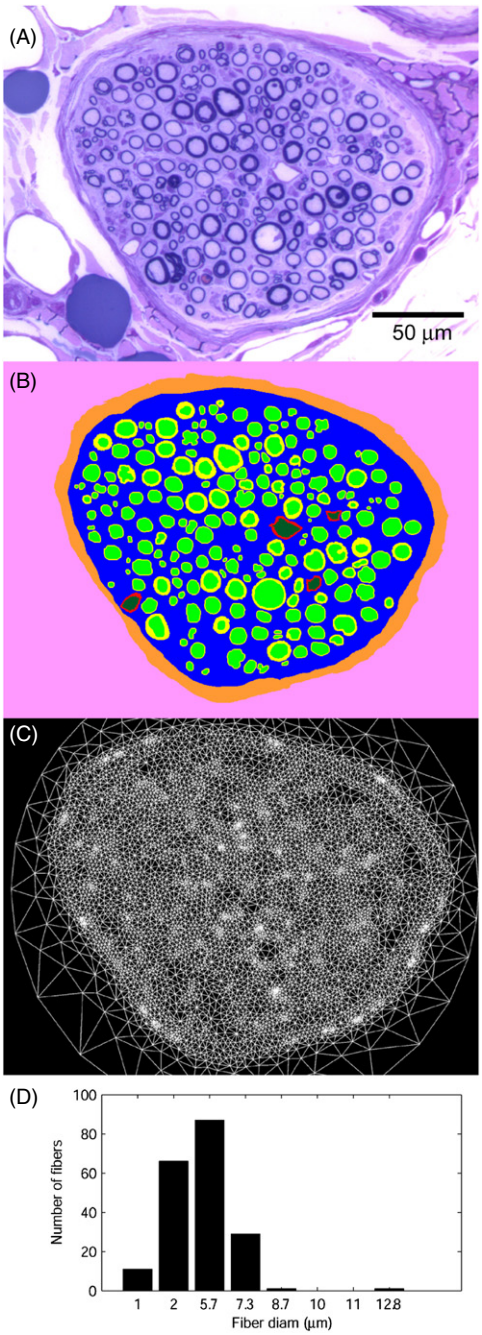

Figure 1. Anatomically derived FEM model. (A) A single fascicle is shown from a stained cross-section of cat sciatic nerve (Richardson stain). (B) The fascicle is artificially re-colored to show several different tissue types: epineurium, perineurium, endoneurium, blood vessel epithelium, blood, axoplasm and myelin. (C) A FEM mesh is constructed from the features in the re-colored image. (D) Fiber size histogram for the myelinated axons in the fascicle.

model (figure 1(A)). This image was re-colored using Adobe Photoshop (Adobe Systems Inc., San Jose, CA) in order to assign one of seven tissue types to each pixel in the cross-section (figure 1(B)). Myelinated fibers were individually identified, and the diameter of each fiber was determined from a circle with the same area. Fiber diameters ranged from .75 to 12.6 μm (figure 1(D)).

Table 1. Tissue conductivities for inhomogeneous model.

Tissue type	Conductivity (S m^{-1})
Endoneurium	0.333
Endothelium	0.6
Blood	0.6
Myelin	1×10^{-6}
Axoplasm	1×10^{-6}[a]
Perineurium	0.01
Epineurium	0.1

[a] See explanation in text.

Bioelectric field model

We used the recolored, anatomical cross-section of the fascicle to construct a 3D finite element model (FEM). First, a 2D, multiresolution mesh of the fascicle image was created using COMSOL 3.1 (Comsol Inc., Burlington, MA). The COMSOL mesh generation library includes specific commands that allow preservation of important features from images. With these functions, we were able to create a mesh that accurately represented the different tissue types and anatomical features of the fascicle (figure 1(C)). The 2D triangulated mesh was then extruded to create a 3D tetrahedral mesh using a custom Matlab program written for that purpose (Mathworks Inc., Natick, MA). The 3D mesh contained 100 copies of the 2D mesh arranged in exponentially increasing slice thicknesses that were symmetric around the $z = 0.0$ plane; the overall volume size was approximately 0.260 mm $\times$ 0.260 mm $\times$ 15 mm. The mesh was imported into BioPSE (Scientific Computing and Imaging Institute 2004), and conductivity tensors were assigned to each tetrahedron.

In order to analyze the differences between isotropic and inhomogeneous tissue, we created two different field models. The former had a single conductivity value assigned to the entire volume, whereas the latter had conductivities assigned on the basis of tissue type and values shown in table 1, which were derived from previous studies. Specifically, Ranck performed a series of experiments to characterize the electrical properties of many physiological materials (Ranck 1963, 1964, Ranck and Bement 1965). Additionally, a compendium was put together by Geddes (Geddes and Baker 1967), and Malmivuo and Plonsey provide a good review of previously reported values (Malmivuo and Plonsey 1995). In order to make meaningful comparisons between the two models, we adjusted the isotropic conductivity until the effective resistance for both tissue models was the same. This was done by using a monopolar current source in the center of the fascicle and adjusting the isotropic conductivity until the voltage difference from source to ground was the same as the inhomogeneous tissue. This resulted in a mean conductivity value of 0.25 S m^{-1} for the isotropic model, a value that is in the range for neural tissue.

Once the 3D model was constructed, current sources and boundary conditions were added. To mimic the effects of a distant return electrode, ground nodes were placed around the outer surface of the FEM mesh. The resulting model was converted into a linear system that was solved using the Poisson equation with a conjugate gradient solver to determine the

potential distribution (V_e) generated within the tissue medium (stiffness matrix σ) resulting from a collection of sources (I):

$$\nabla \cdot \sigma \nabla V_e = -I, \tag{4.1}$$

where ∇ indicates a partial difference with respect to x, y and z. Monopolar and bipolar current source configurations were tested. During monopolar stimulation, the current source was placed in a region of endoneurium located approximately in the center of the nerve. During longitudinal bipolar stimulation, the same location was used in the cross-section, but the two current sources were separated by 200, 500, 750 or 1000 μm along the length of the nerve. During transverse bipolar stimulation, the current sources were separated by 50 μm or 100 μm within the cross-section. Axons were stimulated using a charge-balanced, biphasic waveform with a 250 μs cathodic phase, 100 μs inter-phase interval and a 250 μs anodic phase. This waveform was chosen because it is commonly used for physiological stimulation (McDonnall *et al* 2004a, 2004b).

Threshold detection

One major advantage to FEM-based field models is that they provide solutions to systems with arbitrary geometries. However, one limitation of this approach is that FEM meshes do not easily accommodate features with vastly different spatial scales. This is a relevant problem for modeling neural processes where the axons are approximately three orders of magnitude larger than features such as the nerve membrane, which is on the order of 7 nm in thickness. Although the nerve membrane is not included in the FEM model, consideration of this structure is crucial for accurately determining neural activation. Therefore, two steps were taken. First, the conductivity of axoplasm was reduced to represent the equivalent resistance across the cell membrane and nerve fiber. In a separate series of experiments, this approximation caused errors of less than 1% in the extracellular voltage deflection during worst-case conditions (the peak of the action potential, data not shown). Second, thresholds for neural activation were determined using cable models of myelinated axons that were coupled to the field simulations. Each axon in the anatomical FEM was represented by one of six multi-compartmental cable model axons whose diameters were 1, 2, 5.7, 7.3, 8.7 and 12.8 μm, representing the range of fiber sizes in our sciatic nerve section. The distances between nodes of Ranvier in these fibers were approximately 100 times the fiber diameter, following previously published observations (Rushton 1951): 100, 200, 500, 750, 1000 and 1350 μm, respectively. Because only one 8.7 μm and one 12.8 μm fiber were in the fascicle, results are reported for the remaining fiber sizes. Bioelectric field simulations were coupled to the neural models by interpolating extracellular voltage values onto the corresponding compartments in the cable model neuron. All cable model simulations were performed using neuron (Hines and Carnevale 1997) and were constructed based on a myelinated axon model (McIntyre *et al* 2002). Thresholds were determined by first calculating the field solution from 1 μA cathodic current injection, applying the field to the axons and scaling the voltage up or down until the firing threshold was found using a binary search algorithm. A model neuron was considered to reach threshold when it fired in lockstep with the stimulation waveform for 250 ms. The use of coupled field–neuron simulations provides the best-known accuracy for threshold determination. By contrast, linear methods such as the activating function have substantial limitations in determining thresholds (Moffitt *et al* 2004), although for monopolar stimulation these limitations can be overcome by adjusting the activating function threshold values (Butson and McIntyre 2006). Recruitment curves were generated from the percentage of axons that reached threshold, grouped by model neuron size.

Cable model axons were initially placed such that the centermost node of Ranvier was positioned in the same plane as the cathodic stimulating electrode (0% condition). In order to determine the effects of the position of nodes of Ranvier on activation, neurons were displaced by 25% and 50% of their internodal distance along the length of the fascicle (25% and 50% conditions, respectively).

Electrode configuration

Neural activation as a function of source–neuron distance was determined for monopolar and bipolar electrode configurations. During monopolar stimulation, the current source was placed in an area of endoneurium located roughly in the center of the fascicle. Bipolar stimulation was performed using transverse and longitudinal configurations. Transverse bipolar stimulation was tested for source separation distances of 50 μm or 100 μm. Longitudinal bipolar stimulation was tested for source separation distances of 200, 500, 750 and 1000 μm. In both cases, current sources were centered around the monopolar source position.

Results

Electric field is modulated by tissue properties

We first determined the effects of the conductivity model on the electric field within the tissue medium. After controlling for mean tissue impedance levels, we found that the electric field in the isotropic tissue medium was smooth and radially symmetric, whereas the field generated using the inhomogeneous medium had noticeable variations during monopolar stimulation. These differences are highlighted by examining current streamlines from a monopolar source electrode (figure 2). Streamlines are particularly effective for demonstrating these differences because they show the path of the electric field gradient through the tissue. Across all neurons, voltage differences of up to 20 mV were observed between the different conductivity models. Differences were greater for small source–axon distances, but were roughly the same across all axon diameters after controlling for source–axon distance. More importantly, these differences had a strong effect on neural activation. We found that neural activation thresholds were consistently higher in the isotropic medium for all electrode configurations; the average ratio of isotropic/inhomogeneous threshold current was 2.49 $\pm$ 0.67 (mean $\pm$ standard deviation).

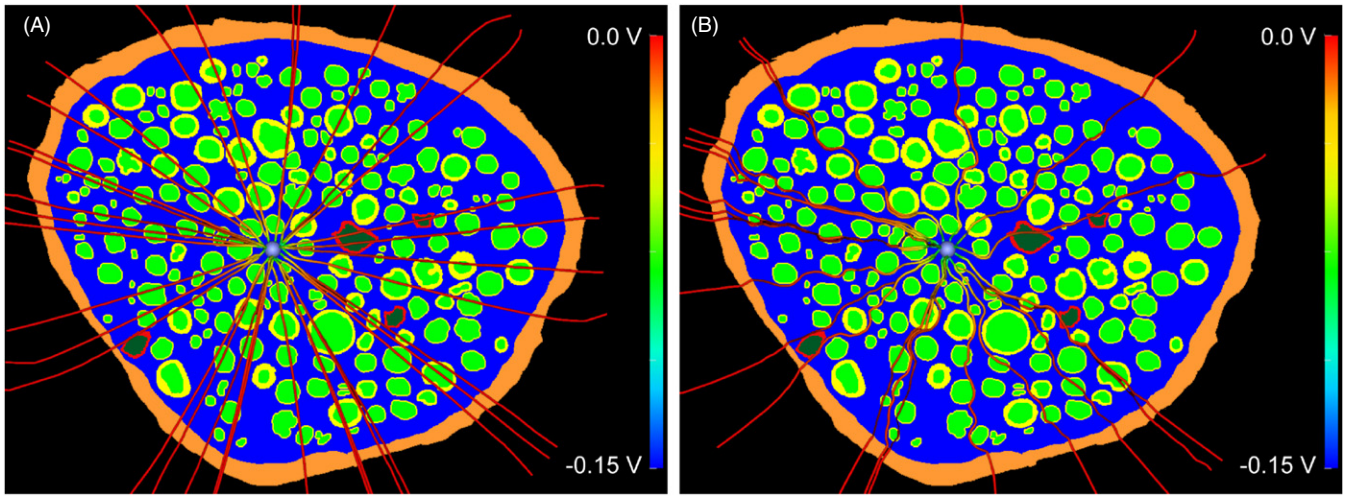

Figure 2. Field solutions. The difference between the (A) isotropic and (B) inhomogeneous field solutions is highlighted using streamlines that are superimposed on the nerve fascicle in this monopolar stimulation example. The streamlines were generated by choosing 15 seed points from the largest vector gradients in the solution and following the electric field from the seed points to ground. Streamlines are colored to indicate voltage according to the bar at right. The fascicle is colored using the same scheme as figure 1(B).

Neural activation is modulated by electrode configuration

We found that it was possible to influence recruitment characteristics by varying the electrode configuration. During monopolar stimulation, the recruitment curves were tightly grouped together and roughly showed the inverse recruitment order commonly observed during extracellular stimulation, at least at higher stimulation values (figure 3). However, it was possible to mitigate this problem through carefully designed bipolar stimulation. Preferential recruitment of a specific fiber populations during longitudinal stimulation was possible by matching the source separation distance to the internodal distance: 1 μm and 2 μm fibers were preferentially activated by a 200 μm source separation; 5.7 μm fibers by a 500 μm separation; and 7.3 μm fibers by a 750 μm separation. We also found that 1000 μm source separation preferentially activated 5.7 μm fibers, indicating that integer multiples of the internodal distance were also effective. In contrast, neither of the transverse bipolar stimulation configurations were effective at attaining physiological recruitment order, but they did cause the slope of the recruitment curve to decrease, a desirable characteristic for motor neuron activation. Interestingly, we observed that the recruitment curves were slightly steeper in the inhomogeneous condition compared with the isotropic condition (data not shown).

Neural activation is modulated by position of nodes of Ranvier

We next determined the degree of variability in neural activation that was caused by the positions of the nodes of Ranvier relative to the current source(s). We found that their positions caused considerable variability in the neural response. The lowest thresholds occurred when the node of Ranvier was aligned with the cathodic current source (0% condition), whereas the highest thresholds were usually (but not always) in the 50% condition. Changes in threshold caused a shift in the recruitment curves, but had little effect on their slope. Threshold variability was also modulated by the electrode configuration (figure 4). During monopolar stimulation, the variability in threshold response was proportional to fiber diameter, with highest variability for the 7.3 μm fiber. For longitudinal electrode configurations, the variability was generally higher for the fiber diameter that was preferentially recruited at that source separation distance. Thus, for example, 7.3 μm fibers showed greater changes in threshold as a function of shifts in internodal distance at a longitudinal source separation distance of 750 μm than at other longitudinal source separation distances. Likewise, 5.7 μm fibers showed greater changes in threshold at longitudinal source separation distances of 500 μm and 1000 μm than at a longitudinal source separation distance of 200 μm. Finally, the highest overall variability occurred in the transverse electrode configurations. The results were qualitatively similar for the isotropic versus inhomogeneous tissue models.

Discussion

Our results show that inclusion of physiologically based tissue properties has a substantial effect on neural activation. The use of isotropic tissue conductivity caused overestimates of the current threshold necessary for activation compared with an inhomogeneous tissue medium. The mechanism for the differences between these models can be partly explained by envisioning the path from source to ground as a voltage divider. In an isotropic medium, each incremental step in distance causes a proportional change in voltage. This is most easily understood for a 1D conductor such as a wire, where the proportionality factor is 1 (for 2D and 3D systems the proportionality factors are $1/r$ and $1/r^2$, respectively, where r is the distance from the source). The inclusion of inhomogeneities such as neurons, blood vessels, epineurium and perineurium in the volume conductor causes voltage

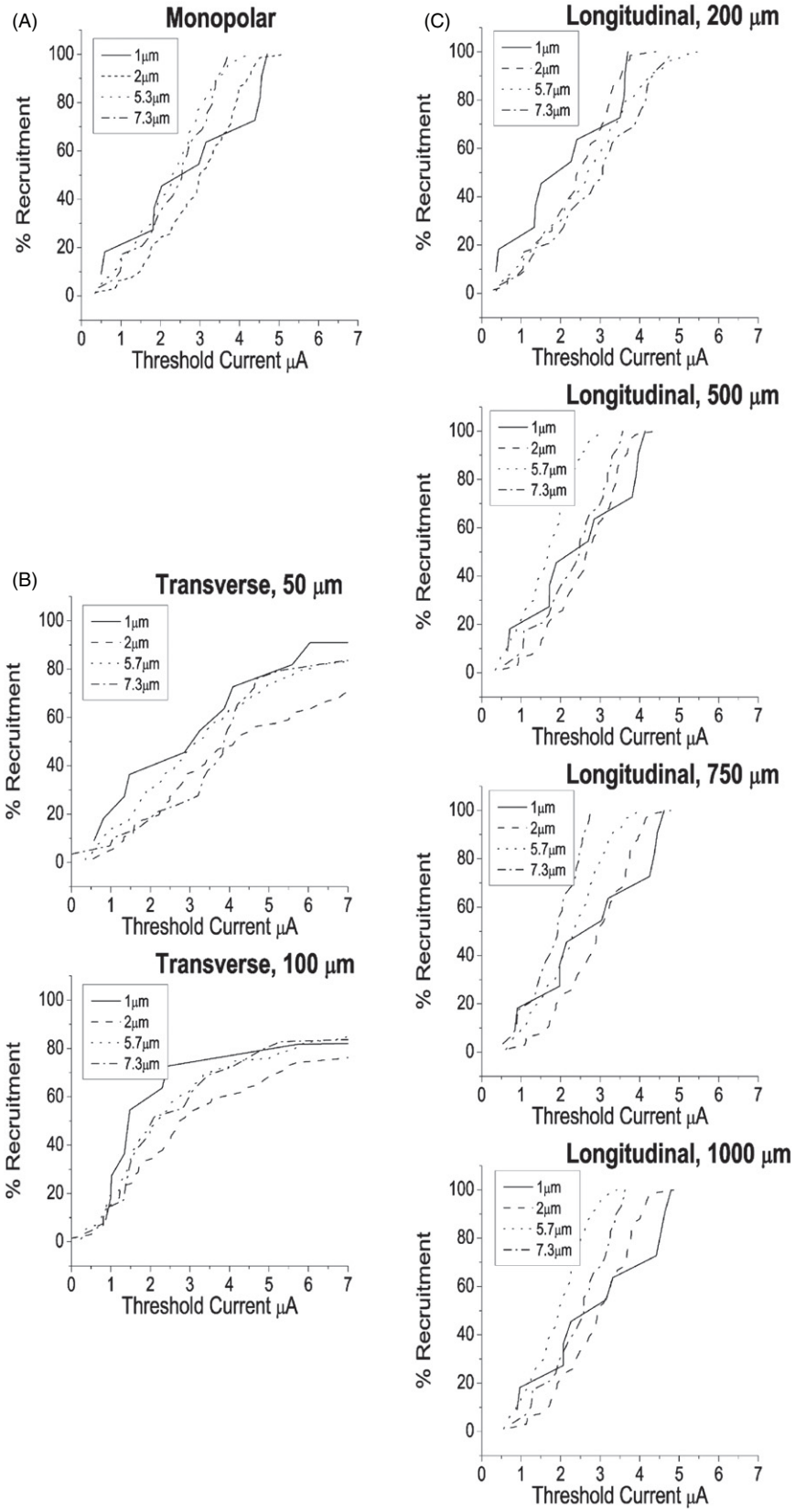

Figure 3. Recruitment curves for different electrode configurations. (A) Monopolar configuration, showing the inverse recruitment order commonly observed during extracellular stimulation. (B) Transverse, bipolar stimulation and (C) longitudinal, bipolar stimulation recruitment curves with source separation distances indicated. Data are shown for inhomogeneous tissue model.

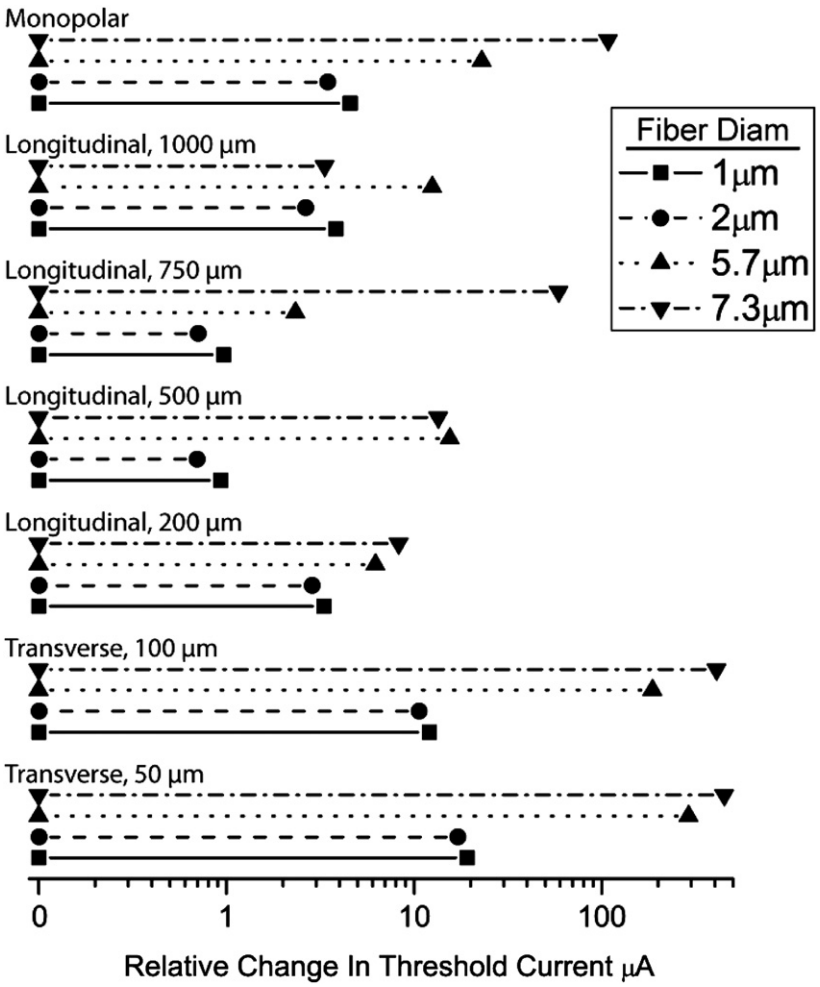

Figure 4. Threshold variability resulting from position of nodes of Ranvier. Data are grouped by electrode configuration, and all data are shown from the 50% position on the recruitment curves in figure 3. Within each electrode configuration, results are shown for axon diameters of 1, 2, 5.7 and 7.3 μm. For each fiber diameter, relative changes in threshold current are shown as a function of displacement of nodes of Ranvier from 0% (aligned in the same cross-sectional plane with the cathodic electrode) to 50% internodal shifts.

profiles that differ from the isotropic model: in regions of high conductivity the voltage falls off more slowly, and in regions of low conductivity the voltage falls off more rapidly. In a 3D model, these inhomogeneities cause complex variations in the electric field as exemplified in figure 2. The inclusion of nodes of Ranvier into the tissue model caused large variability in threshold responses, and this variability was modulated by the fiber diameter and the current source configuration. These results suggest that the variable positions of the nodes of Ranvier create a lower bound on the precision with which different fiber populations can be activated. Rather than exclusively targeting a single group of fibers, it is more realistic to bias the activation toward specific fiber sizes, but with substantial overlap to other populations.

The fiber sizes included in these experiments were chosen based on their presence in the histological slice, and most likely represent both efferent and afferent functional groups. Larger fibers are likely part of efferent motor groups, while smaller fibers could include afferents mediating sensations such as temperature and pain. Presently available histological techniques preclude us from discriminating efferent from afferent fibers. Such discrimination is equally imprecise during FES, which is why undesirable sensations are a common side effect. However, the information provided in the results could be used to select stimulation motifs that activate, or to avoid activation in particular fiber groups. In this regard it is noteworthy that the recruitment curves reflect activation characteristics that could be peculiar to intraneural stimulation. For example, figure 3(A) shows that the smallest fibers have higher recruitment percentages at lower current amplitudes, which may seem contradictory to previous observations regarding recruitment order during extraneural stimulation (e.g. larger fibers before smaller fibers). This feature could be attributable to the fact that smaller diameter fibers have shorter internodal spacing and less variability in firing threshold due to alignment of nodes of Ranvier relative to the cathodic electrode (as illustrated in figure 4), resulting in a bias toward such fibers at low stimulus amplitudes. However, it is also possible that the modest number of fibers in the 1 μm group may cause recruitment to be disproportionately represented by activation of a few individual axons.

Two desirable characteristics of neural stimulation systems are fiber size selectivity and shallow recruitment curves. The former allows for greater control over the size

of the motor unit activated due to the correlation between axon diameter and muscle motor unit size. In turn, this provides greater control over the strength and precision of the motor response and may allow selective activation of fatigue-resistant motor units. The latter is desirable for attaining finer gradations in muscle response for an incremental increase in stimulation current. Our results suggest that these goals may be accomplished with a carefully designed electrode array, and that there may be more effective designs than planar arrays with fixed spacing in the x and y directions. For example, a better configuration might be to provide variable spacing in the longitudinal direction to match the internodal distance of the target fiber populations. With the use of high-density arrays, improved selectivity of activation might also be achieved via the choice of electrodes with the appropriate spacing. Further, the use of transverse stimulation in combination with targeting specific fiber populations could produce a shallower recruitment curve.

Researchers have used a variety of methods to determine neural activation thresholds. For example, Warman *et al* (1992) developed a method for predicting neural activation based on the second difference of the extracellular voltage profile along the neural process. This method is adequate for determining neural activation as long as accurate thresholds can be determined (Butson and McIntyre 2006). The major advantage of this method is the drastically reduced computational cost compared with cable model simulations. However, this method is difficult to generalize for complex extracellular voltage profiles and can result in substantial errors (Moffitt *et al* 2004). An alternative method that directly accounts for the detailed biophysics of the nerve and accommodates the complex field changes resulting from arbitrary electrode configurations is the coupled field–neuron simulations used to generate these results.

Any type of charge injection into biological tissue must conform to safe stimulation limits to prevent tissue damage. Chronic electrical stimulation of the nervous system requires the use of biphasic, charge-balanced waveforms to prevent tissue damage and electrode corrosion (Pudenz *et al* 1975). Another safety consideration is the current density at the electrode surface. Although we do not explicitly include stimulating electrodes in our bioelectric field model, the configuration of current sources studied in this paper are modeled after the Utah Electrode Array, which is a micro-machined silicon array of point electrodes, each of which is approximately 80 μm wide at its base and tapers to a sharpened tip with a radius of 1–4 μm, with a surface area of roughly 1250 μm^2 (Branner and Normann 2000). Electrodes with such small surface area generally have higher current densities than larger electrodes, and in this case there are two primary concerns. First, Shannon developed a model for predicting safe levels of electrical stimulation (Shannon 1992) based on previously published empirical data (McCreery *et al* 1990):

$$\log(\mathrm{CD}) = k - \log(Q), \tag{4.2}$$

where CD is the charge density in $\mu C/cm^2$/phase and Q is the charge in μC/phase and k is a proportionality constant. This provided estimates for safe stimulation limits using disk electrodes with $k = 1.5$, and these values have been widely accepted. However, the supporting data were from experiments conducted for a short period of time (7 h) at 50 Hz, and we do not yet know how to extrapolate these values for longer stimulation durations or different frequencies. Shannon took this analysis a step further by proposing a model that would take into account edge effects of the electrode (i.e. nonuniform current densities across the electrode surface) and the position of the neural elements relative to the electrode. Other results from stimulation-induced damage using microelectrodes suggest that $k = 0.75$ is a more appropriate limit (McIntyre and Grill 2001). Second, for electrodes with small surface area there is a possibility of gas evolution at the electrode–tissue interface, which is undesirable due to its corrosive effects. The Utah Array uses iridium electrodes contacts that are oxidized to increase the charge carrying capacity. With this modification, higher current amplitudes are possible before gas evolution occurs.

Although every effort was made to represent accurately the physiological properties of the nerve fascicle with the model, the model contains a number of assumptions and limitations. First, the model does not take into account changes in the electric field that would occur as a result of trans-membrane axonal currents. Prior experiments have show that this effect is small, causing voltage changes of less than 1% in the surrounding tissue. Hence, this is not considered a major source of error. Second, the axon models used in this study are highly detailed and able to reproduce a wide range of experimentally measured excitation characteristics. However, they are general models of myelinated neurons that may differ from the specific characteristics of peripheral motor neurons. Further, some error is introduced by representing the range of fiber sizes shown in figure 1 by six model neurons. Third, the differences between the isotropic and inhomogeneous models will likely be greater with the inclusion of additional anatomical features. For example, the model does not include unmyelinated fibers that are not visible using the Richardson staining method. Inclusion of these fibers would further disrupt the symmetry of the field solution, and would likely cause additional differences in activation thresholds. Lastly, the electrode–tissue interface can have substantial effects on neural activation. We did not explicitly include the electrode in the FEM mesh or the electrode–tissue interface in the biophysical model, and these will both likely increase activation thresholds. Rather, electrodes were represented by idealized current sources, which have been shown to be good approximations of electrodes for distances greater than 50 μm (McIntyre and Grill 2001). However, the purpose of this paper was to isolate specific features of the physiology in order to examine the effects of physiologically based tissue properties on activation in a controlled environment, and the model is appropriate for that purpose.

The results of this study show that the physiological properties of the tissue medium and the morphological properties of the individual neurons exert considerable influence on the neural response. These results are not captured by isotropic conductivity models with simplified threshold measurement methods such as the activating

function. The results suggest ways to achieve selective activation with carefully controlled electrode spacing, and provide new insights into the body–machine interface component of neuromuscular FES systems.

References

Branner A and Normann R A 2000 A multielectrode array for intrafascicular recording and stimulation in sciatic nerve of cats *Brain Res. Bull.* **51** 293–306

Brill N, Polasek K, Oby E, Ethier C, Miller L and Tyler D 2009 Nerve cuff stimulation and the effect of fascicular organization for hand grasp in nonhuman primates *Conf. Proc. IEEE Eng. Med. Biol. Soc. 2009* pp 1557–60

Butson C R and McIntyre C C 2006 Role of electrode design on the volume of tissue activated during deep brain stimulation *J. Neural. Eng.* **3** 1–8

Dowden B R, Wark H A and Normann R A 2010 Muscle-selective block using intrafascicular high-frequency alternating current *Muscle Nerve* **42** 339–47

Dowden B R, Wilder A M, Hiatt S D, Normann R A, Brown N A and Clark G A 2009 Selective and graded recruitment of cat hamstring muscles with intrafascicular stimulation *IEEE Trans. Neural Syst. Rehabil. Eng.* **17** 545–52

Durand D, Park H J and Wodlinger B 2009 Models of the peripheral nerves for detection and control of neural activity *Conf. Proc. IEEE Eng. Med. Biol. Soc. 2009* pp 3326–9

Geddes L A and Baker L E 1967 The specific resistance of biological material—a compendium of data for the biomedical engineer and physiologist *Med. Biol. Eng.* **5** 271–93

Grill W M Jr 1999 Modeling the effects of electric fields on nerve fibers: influence of tissue electrical properties *IEEE Trans. Biomed. Eng.* **46** 918–28

Grill W M Jr and Mortimer J T 1996 The effect of stimulus pulse duration on selectivity of neural stimulation *IEEE Trans. Biomed. Eng.* **43** 161–6

Grill W M and Mortimer J T 1997 Inversion of the current–distance relationship by transient depolarization *IEEE Trans. Biomed. Eng.* **44** 1–9

Grinberg Y, Schiefer M A, Tyler D J and Gustafson K J 2008 Fascicular perineurium thickness, size, and position affect model predictions of neural excitation *IEEE Trans. Neural Syst. Rehabil. Eng.* **16** 572–81

Hambrecht F T and Reswick J B 1977 *Functional Electrical Stimulation: Applications in Neural Prostheses* (New York: Dekker)

Hines M L and Carnevale N T 1997 The NEURON simulation environment *Neural Comput.* **9** 1179–209

Johnson C R 1997 Computational and numerical methods for bioelectric field problems *Crit. Rev. Biomed. Eng.* **25** 1–81

Lertmanorat Z and Durand D M 2004a A novel electrode array for diameter-dependent control of axonal excitability: a simulation study *IEEE Trans. Biomed. Eng.* **51** 1242–50

Lertmanorat Z and Durand D M 2004b Extracellular voltage profile for reversing the recruitment order of peripheral nerve stimulation: a simulation study *J. Neural Eng.* **1** 202–11

Malmivuo J and Plonsey R 1995 *Bioelectromagnetism: Principles and Applications of Bioelectric and Biomagnetic Fields* (New York: Oxford University Press)

McCreery D B, Agnew W F, Yuen T G and Bullara L 1990 Charge density and charge per phase as cofactors in neural injury induced by electrical stimulation *IEEE Trans. Biomed. Eng.* **37** 996–1001

McDonnall D, Clark G A and Normann R A 2004a Interleaved, multisite electrical stimulation of cat sciatic nerve produces fatigue-resistant, ripple-free motor responses *IEEE Trans. Neural Syst. Rehabil. Eng.* **12** 208–215

McDonnall D, Clark G A and Normann R A 2004b Selective motor unit recruitment via intrafascicular multielectrode stimulation *Can. J. Physiol. Pharmacol.* **82** 599–609

McIntyre C C and Grill W M 2001 Finite element analysis of the current-density and electric field generated by metal microelectrodes *Ann. Biomed. Eng.* **29** 227–35

McIntyre C C, Richardson A G and Grill W M 2002 Modeling the excitability of mammalian nerve fibers: influence of afterpotentials on the recovery cycle *J. Neurophysiol.* **87** 995–1006

McNeal D R 1976 Analysis of a model for excitation of myelinated nerve *IEEE Trans. Biomed. Eng.* **23** 329–37

Moffitt M A, McIntyre C C and Grill W M 2004 Prediction of myelinated nerve fiber stimulation thresholds: limitations of linear models *IEEE Trans. Biomed. Eng.* **51** 229–36

Normann R A 2007 Technology insight: future neuroprosthetic therapies for disorders of the nervous system *Nat. Clin. Pract. Neurol.* **3** 444–52

Peckham P H and Gray D B 1996 Functional neuromuscular stimulation (FNS) *J. Rehabil. Res. Dev.* **33** ix–xi

Pudenz R H, Bullara L A, Jacques S and Hambrecht F T 1975 Electrical stimulation of the brain: III. The neural damage model *Surg. Neurol.* **4** 389–400

Ranck J B Jr 1963 Specific impedance of rabbit cerebral cortex *Exp. Neurol.* **7** 144–52

Ranck J B Jr 1964 Specific impedance of cerebral cortex during spreading depression, and an analysis of neuronal, neuroglial and interstitial contributions *Exp. Neurol.* **9** 1–16

Ranck J B Jr and Bement S L 1965 The specific impedance of the dorsal columns of cat: an inisotropic medium *Exp. Neurol.* **11** 451–63

Rushton W A 1951 A theory of the effects of fibre size in medullated nerve *J. Physiol.* **115** 101–22

Schiefer M A, Triolo R J and Tyler D J 2008 A model of selective activation of the femoral nerve with a flat interface nerve electrode for a lower extremity neuroprosthesis *IEEE Trans. Neural Syst. Rehabil. Eng.* **16** 195–204

Scientific Computing and Imaging Institute 2004 'BioPSE' the biomedical problem solving environment http://software.sci.utah.edu/biopse.html

Shannon R V 1992 A model of safe levels for electrical stimulation *IEEE Trans. Biomed. Eng.* **39** 424–6

Veltink P H, Van Veen B K, Struijk J J, Holsheimer J and Boom H B 1989 A modeling study of nerve fascicle stimulation *IEEE Trans. Biomed. Eng.* **36** 683–92

Warman E N, Grill W M and Durand D 1992 Modeling the effects of electric fields on nerve fibers: determination of excitation thresholds *IEEE Trans. Biomed. Eng.* **39** 1244–54

Wieler M, Stein R B, Ladouceur M, Whittaker M, Smith A W, Naaman S, Barbeau H, Bugaresti J and Aimone E 1999 Multicenter evaluation of electrical stimulation systems for walking *Arch. Phys. Med. Rehabil.* **80** 495–500